A peer-reviewed version of this preprint was published in PeerJ on 17 March 2015.

Stewart SB, Koller JM, Campbell MC, Perlmutter JS, Black KJ. 2015. Additive global cerebral blood flow normalization in arterial spin labeling perfusion imaging. PeerJ 3:e834 https://doi.org/10.7717/peerj.834

Additive global cerebral blood flow normalization in arterial spin labeling perfusion imaging

Stephanie B. Stewart, MD (Depts. of Neurology and Psychiatry)

Jonathan M. Koller, BSBME, BSEE (Dept. of Psychiatry)

Meghan C. Campbell, PhD (Depts. of Neurology and Radiology)

Joel S. Perlmutter, MD (Depts. of Neurology, Radiology, and Anatomy & Neurobiology, Division of Biology and Biomedical Sciences, and Programs in Physical Therapy and Occupational Therapy)

Kevin J. Black, MD (Depts. of Psychiatry, Neurology, Radiology, Anatomy & Neurobiology, and Division of Biology and Biomedical Sciences)

Washington University School of Medicine, St. Louis, MO 63110, USA

Direct correspondence to Dr. Black:

Campus Box 8134

Department of Psychiatry

660 S. Euclid Ave.

St. Louis, MO 63110-1093

Telephone: (314) 362-5041

Fax: (314) 362-0168

kevin@WUSTL.edu

Acknowledgement

The data came from a study funded by Synosia Therapeutics. The analysis reported here was supported by NIH (K24 MH087913 and T32 DA007261).

PeerJ PrePrints | http://dx.doi.org/10.7287/peerj.preprints.464v3 | CC-BY 4.0 Open Access | rec: 11 Sep 2014, publ: 11 Sep 2014

Abstract

To determine how different methods of normalizing for global cerebral blood flow (gCBF) affect image quality and sensitivity to cortical activation, pulsed arterial spin labeling (pASL) scans obtained during a visual task were normalized by either additive or multiplicative normalization of modal gCBF. Normalization by either method increased the statistical significance of cortical activation by a visual stimulus. However, image quality was superior with additive normalization, whether judged by intensity histograms or by reduced variability within gray and white matter.

Keywords

arterial spin labeling; ASL; cerebral blood flow; cerebral blood flow measurement; functional magnetic resonance imaging; fMRI; Parkinson's disease

Introduction

Blood flow imaging of the brain has brought insights to neuroscience for over 50 years (Taber et al. 2005). Whole-brain, or global, cerebral blood flow (gCBF) calculated from blood flow images can be the outcome measure of interest, or can permit correction for gCBF fluctuations that complicate identifying or interpreting relative changes in regional blood flow (rCBF) (Black et al. 2002a).

Early *in vivo* measures of CBF in humans used PET to collect an autoradiographic image of radioactive counts over a defined interval of time (Herscovitch et al. 1983). Measuring arterial radioactivity over time allowed calculation of quantitative rCBF from the PET image of radioactivity concentration (Herscovitch et al. 1983; Raichle et al. 1983). Changes in rCBF then could be calculated by subtracting two different PET images of rCBF. Many PET activation studies accounted for fluctuations of gCBF between PET scans without measuring of an arterial input function by multiplicatively scaling global PET counts (Fox et al. 1984).

By contrast, perfusion images from arterial spin labeling (ASL) MRI are created by subtracting two images obtained a few seconds apart, one in which arterial blood flowing into the brain has been labeled using a spatially limited radio frequency pulse ("tag") and a second image without that label ("control") (Wang et al. 2003). Subtraction creates the possibility of a negative or positive additive bias across a CBF image, in which case additive rather than multiplicative correction may better equalize the intensity of two ASL CBF images.

In 2008 we performed an ASL pharmacological challenge MRI study in Parkinson disease (PD) (Black et al. 2010b). The original analysis scaled the images multiplicatively based on our experience with PET blood flow

PeerJ PrePrints | http://dx.doi.org/10.7287/peerj.preprints.464v3 | CC-BY 4.0 Open Access | rec: 11 Sep 2014, publ: 11 Sep 2014

imaging (Black et al. 2002b). However, when we revisited those images recently for a new analysis (Stewart et al. 2014), the voxel values of the scaled images suggested that additive rather than multiplicative correction might be superior. We test that hypothesis here using several criteria to assess image quality.

Material & Methods

Study participants

Twenty-one nondemented, nondepressed, ambulatory adults age 40–75 with idiopathic PD, treated with a stable dose of levodopa but no dopamine agonists, participated in the study. Detailed inclusion and exclusion criteria and subject characteristics were reported previously (Black et al. 2010a; Black et al. 2010b). Subjects were enrolled in a Phase 2a dose-finding study (Black et al. 2010b), but here we use only data acquired on the placebo day when subjects were in the "practical off state" (*i.e.* no antiparkinsonian medications for at least 9 hours). The study was approved by the Washington University Human Research Protection Office (IRB), and all subjects provided written documentation of informed consent prior to participation.

Subject behavior

Each scanning session included two perfusion MRI scans while the subject fixated a central crosshair surrounded by a circular checkerboard reversing at 8Hz and two control visual fixation scans with the crosshair but no checkerboard.

MR image acquisition

All MRI data were acquired on a Siemens 3T Tim Trio with matrix head coil. ASL images were acquired with the commercial Siemens pulsed arterial spin labeling (pASL) sequence (Wang et al. 2003). Fifteen transverse echo-planar readout slices were acquired with center-to-center slice distance 7.5 mm, 64×64 voxels in plane with dimensions $(3.4375\text{mm})^2$, repetition time (TR) 2.6 sec, echo time (TE) 13.0 msec, and flip angle 90°. An M_0 image was followed by 31 tag-control pairs for a total acquisition time for each ASL "scan" of 2.73 min.

Brain structure was assessed from sagittal MP-RAGE acquisitions with voxel size $(1.0\text{mm})^3$, TR = 2.4 sec, TE = 3.08 msec, TI = 1000 msec, flip angle = 8°. The structural images for each subject were inspected visually, images of lower quality were rejected, and the remaining 1–4 MP–RAGE images for each subject were mutually registered.

Image registration and creation of CBF images

The 63 frames of the ASL run were rigidly aligned using a validated method (Black et al. 2001) and summed to facilitate later alignment steps. Each frame was smoothed using a Gaussian filter with 7.35mm kernel

PeerJ PrePrints | http://dx.doi.org/10.7287/peerj.preprints.464v3 | CC-BY 4.0 Open Access | rec: 11 Sep 2014, publ: 11 Sep 2014

(FWHM), and cerebral blood flow (CBF) was computed in each voxel for each tag-control pair as described (Wang et al. 2003). The summed, aligned EPI images from each run were mutually aligned within each subject and summed across runs, and the resulting image was affine registered to a target image in Talairach and Tournoux space made using validated methods from the structural MR images from these subjects (Black et al. 2004). The products of the registration matrix from this step and the matrices from the within-run mutual registration step were used to resample the 31 tag-control pair CBF images from each run into atlas space in a single resampling step. A whole-brain binary image was created from the atlas-space structural target image, and all analyses below included only the CBF image voxels corresponding to voxels within this mask image.

To minimize motion-related artifact we removed tag–control pairs from all further analyses if framewise displacement in either EPI image exceeded 0.9mm as defined by Siegel et al (2014). The remaining CBF images in atlas space were averaged to create a single atlas-registered CBF image for each ASL run. One subject's data was excluded from further analysis because over half of the frame pairs were removed due to head motion.

Image intensity correction

Estimating modal CBF image intensity

The image intensity histograms were constructed with bins 1 unit wide, so were not smooth. We chose to normalize image intensity based on the idealized peak of this distribution (which if there were no noise would be the mode, *i.e.* the most common voxel intensity in the brain) (Ojemann et al. 1997). Specifically, the method of least squares was used to identify the vertex of the parabola that best fit the histogram using voxels within 70% of the mode bin (Suppl. Fig. 1).

Additive and multiplicative intensity correction

Each input image was corrected in two ways: multiplicatively (multiplying every voxel in the image by 50/*mode*), and additively (adding 50-*mode* to every voxel), so that the idealized modal CBF for every corrected image was 50 (nominal units mL/hg/min).

Defining volumes of interest

Gray matter (GM), white matter (WM) and visual cortex volumes of interest (VOIs) were defined from each subject's high-resolution MP-RAGE image by FreeSurfer (version 5.3, http://surfer.nmr.mgh.harvard.edu) (Desikan et al. 2006). VOIs were limited to voxels that were represented in every image in every subject; this step excluded much of the inferior occipital cortex in the visual cortex VOI (Black et al. 2010b).

PeerJ PrePrints | http://dx.doi.org/10.7287/peerj.preprints.464v3 | CC-BY 4.0 Open Access | rec: 11 Sep 2014, publ: 11 Sep 2014

Statistical analysis

To determine the effect of gCBF normalization on task effect, all statistical analyses were performed in triplicate, one for each set of images: uncorrected (before removing the gCBF effect), multiplicatively normalized, and additively corrected.

Image quality analysis

Using only the fixation scans, the mean rCBF and its variability in the GM and WM Freesurfer-defined VOIs was determined. The gray to white matter ratio was also calculated. The within subject variability in the GM and WM VOIs was also determined.

VOI analysis

To determine the change in rCBF in a VOI with visual stimulation, the mean CBF across all voxels in the VOI from the fixation scans was subtracted from the corresponding mean in the task scans. Statistical significance was assessed with paired t tests.

Statistical images

To identify regions activated by the visual task, we used a mixed-effects approach. First, for each study subject, changes in rCBF were identified using SPM12b software (www.fil.ion.ucl.ac.uk/spm/) and a voxelwise general linear model that included task (checkerboard) *vs.* control (fixation). A t image for each subject was generated from the task contrast. These single-subject t images were used as input for a second SPM analysis using a voxelwise general linear model that included a covariate for subject age and a factor for sex. Statistical inference was performed at each voxel with a one-sample t test (*i.e.* testing whether the task contrast images are significantly less than or greater than zero, across subjects). After thresholding at $t = 3.646$ ($p<0.001$), multiple comparisons correction was performed with the cluster false discovery rate set at $p = 0.05$. Approximate anatomical locations of peaks in the statistical images were provided by the Talairach Daemon client (www.talairach.org) (Lancaster et al. 2000).

Results

We assessed the effect of additive or multiplicative intensity equalization in several ways: by examining the voxel intensity distribution (by frequency histogram), by judging image quality visually, by the variability of voxel intensity within the GM and WM, and by the suitability of each set of images for detecting appropriate brain activation with visual stimulation.

Voxel intensity distribution (histogram)

The idealized mode ± SD for the original CBF images was 33.36 ± 7.30. The original CBF images contained a

PeerJ PrePrints | http://dx.doi.org/10.7287/peerj.preprints.464v3 | CC-BY 4.0 Open Access | rec: 11 Sep 2014, publ: 11 Sep 2014

reasonable distribution of voxel intensities except that many of them appeared shifted leftwards to varying degrees, so that many voxels in the brain had physiologically impossible negative values (the 3 curves in the histogram in the first row of Fig. 1 reflect all brain voxels from 3 successive ASL images from the same subject; a transverse section from each of these images is shown to the right of the histogram). Multiplicative normalization of course produced an image with an equal fraction of negative voxel values, though the normalized image's mode was now 50 (histograms in second row of Fig. 1). Additive normalization produced a voxel intensity distribution that reflects the physiological expectation. In addition, it much more accurately matches the intensity distribution widths across the normalized images (histograms in third row of Fig. 1).

PeerJ PrePrints | http://dx.doi.org/10.7287/peerj.preprints.464v3 | CC-BY 4.0 Open Access | rec: 11 Sep 2014, publ: 11 Sep 2014

Figure 1. Additive intensity normalization improves pASL image quality

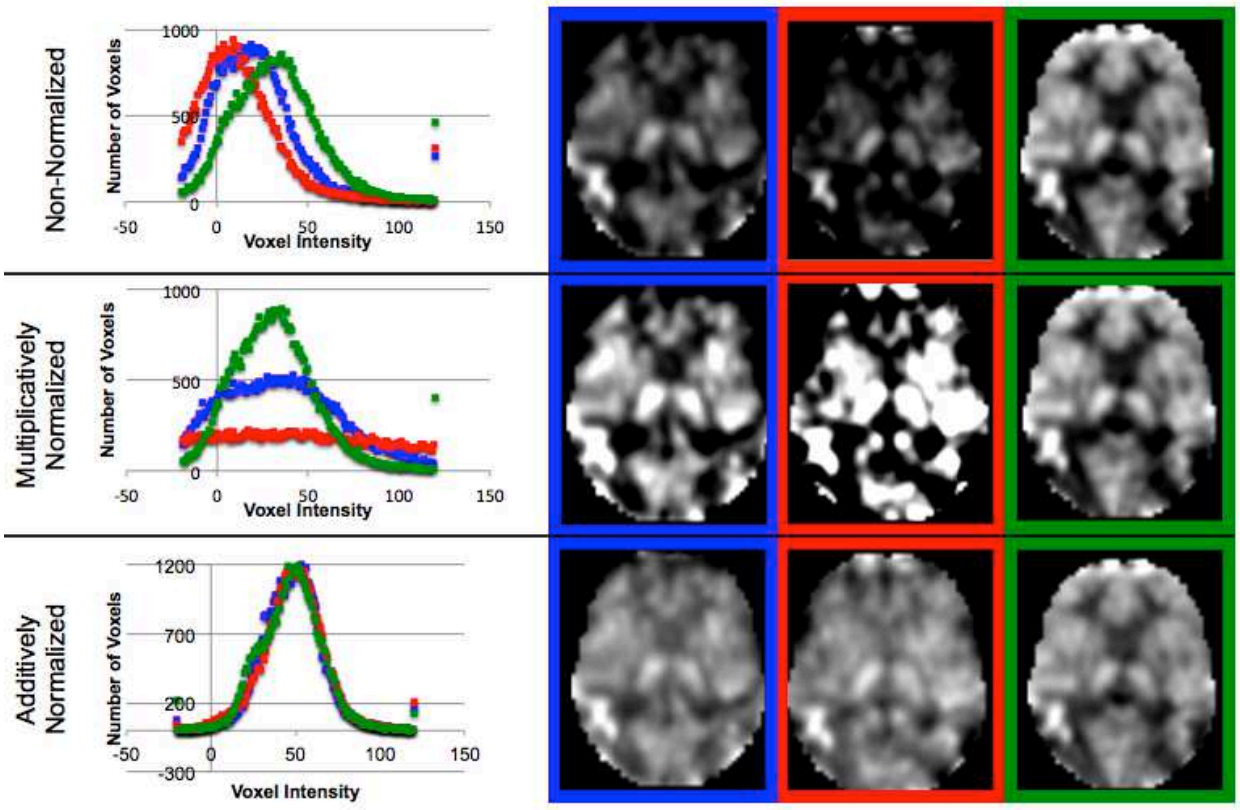

Fig. 1. The effect of multiplicative or additive intensity normalization on 3 ASL scans (represented by red, blue and green) from a single subject. Top row: before normalization, middle row: after multiplicative normalization, bottom row: after additive normalization. The first column shows frequency histograms of the voxel values across the brain (*i.e.* within an anatomically-defined brain mask only) for each of the 3 scans. The remaining columns show the same transverse slice in atlas space from the 3 scans; the image in the 2nd column corresponds to the histogram points marked in blue; similarly the 3rd column in red and the 4th column in green. The grayscale range is set at 0–100ml/hg/min, a range that reasonably reflects true physiological values, except for the images on the top row, for which the range is set at 0–75ml/hg/min because otherwise the structure in some of the images would be obscured.

Image quality

Images normalized additively (third row in Fig. 1) appear to show more uniform voxels within the GM and WM. To corroborate this quantitatively, we determined the variability in the GM and WM both between subjects and within subjects, using scans from the fixation task only.

PeerJ PrePrints | http://dx.doi.org/10.7287/peerj.preprints.464v3 | CC-BY 4.0 Open Access | rec: 11 Sep 2014, publ: 11 Sep 2014

Across subjects, the mean GM intensities are more similar in additively normalized scans (coefficient of variability [CV] = 0.145) as compared to non-normalized (CV=0.194) or multiplicatively normalized scans (CV=0.266). The WM intensities are also more similar in additively normalized scans (CV=0.158; non-normalized CV=0.206, multiplicatively normalized scans CV=0.263). The GM:WM ratio is also more similar across subjects after additive normalization (CV=0.056; non-normalized CV=0.074, multiplicatively normalized CV=0.072) (Suppl. Table 1).

Within subjects, additively normalized scans had less variability within GM (within-subject CV 0.141, averaged across subjects) as compared to multiplicatively normalized images (mean CV 0.217), and the same was true for WM (mean CV 0.141 *vs.* 0.211) (Suppl. Table 2).

Task activation: a priori *volume of interest*

We examined the effect of visual stimulation in the partial visual cortex VOI (intended as a positive control) and in the WM VOI (intended as a negative control). With this substantial visual stimulus, the signal is detected even without normalization (visual cortex VOI, $p=1.70 \times 10^{-5}$, paired t test), but the statistical significance of the change is greater in either set of normalized images (multiplicative normalization, $p=1.03 \times 10^{-6}$, additive normalization, $p=7.72 \times 10^{-6}$). The mean change in rCBF in the visual cortex VOI increased when the images were multiplied, but was always >10 times higher than the change in the WM control VOI (Suppl. Table 3).

Task activation: statistical image

Similarly to the VOI analysis, with this substantial visual stimulus, SPM analyses of visual stimulation identified significant occipital cortex activation even without normalization, though normalization increased the peak t and the volume of significant clusters (see Table 1). For all 3 analyses, the peak t value occurs in the occipital lobe, in Brodmann area 17 or 18.

PeerJ PrePrints | http://dx.doi.org/10.7287/peerj.preprints.464v3 | CC-BY 4.0 Open Access | rec: 11 Sep 2014, publ: 11 Sep 2014

Table 1: Activation by a visual stimulus: SPM analyses

	Non-normalized Images	Multiplicatively Normalized	Additively Normalized
peak t (17 d.f.)	6.13	7.36	6.48
location of peak	-8, -93, 6	4, -81, 0	-8, -93, 6
cluster volume, voxels (ml)	119 (3.2)	369 (10.0)	447 (12.1)
p (FDR)	<0.0005	<0.0005	<0.0005
peak t for 2nd significant cluster	5.59		
location of peak	26, -87, 9		
cluster volume, voxels (ml)	247 (6.7)		
p (FDR)	<0.0005		

Discussion

Additive normalization of gCBF is superior to multiplicative normalization for this pASL technique, judged by image intensity distributions and by homogeneity within gray matter and white matter. Multiplicative scaling increases the variability in GM and WM, whereas additive normalization improves image quality and reduces variability within and between subjects.

The reader familiar with ASL should note a different and potentially confusing use of the term "global." Before calculating CBF, several pre-processing quality improvement steps are applied to the EPI images to address signal artifacts caused by head movement or MR signal drift over time within an ASL run. Wang (2012) used a general linear model and global EPI signal intensity (defined by voxels above an arbitrary intensity threshold) to account for such artifactual signal changes. We chose to address these issues using methods developed and validated at our institution; for instance, we removed motion-contaminated frames (Siegel et al. 2014) rather than modeling the consequent artifact. Wang's within-run global signal variable is quite different from the global (whole-brain) measurement of CBF compared between runs in this communication.

We previously found that correcting for gCBF improved task signal in ASL in young, healthy volunteers (Black et al. 2008; Henniger et al. 2009). The present report extends those findings to patients with Parkinson disease. Normalizing scans for variability in gCBF improves detection of statistically significant activations from a visual task, whether analyzed using an anatomically-defined visual cortex VOI or by whole-brain SPM. Although noise properties improve to a greater extent with additive scaling, either additive or multiplicative scaling permits identification of rCBF responses to a strong visual stimulus.

PeerJ PrePrints | http://dx.doi.org/10.7287/peerj.preprints.464v3 | CC-BY 4.0 Open Access | rec: 11 Sep 2014, publ: 11 Sep 2014

Disclosure/Conflict-of-Interest Statement

The original study was funded commercially, but the sponsor did not participate in or affect this analysis or this report. There have been no other commercial or financial relationships that could be construed as a potential conflict of interest.

References

Black KJ, Campbell MC, Dickerson W, Koller JM, Chung SC, and Bandak SI. 2010a. A randomized, double-blind, placebo-controlled cross-over trial of the adenosine 2a antagonist SYN115 in Parkinson disease. Annual meeting of the American Academy of Neurology. Toronto, CA.

Black KJ, Duvall LB, Campbell MC, and Koller JM. 2008. Signal and noise in continuous arterial spin labeling (cASL) as a function of time. Annual meeting, Society for Neuroscience. Washington, DC. p Program # 598.593.

Black KJ, Hershey T, Koller JM, Videen TO, Mintun MA, Price JL, and Perlmutter JS. 2002a. A possible substrate for dopamine-related changes in mood and behavior: prefrontal and limbic effects of a D_3-preferring dopamine agonist. *Proceedings of the National Academy of Sciences of the United States of America* 99:17113-17118.

Black KJ, Hershey T, Koller JM, Videen TO, Mintun MA, Price JL, and Perlmutter JS. 2002b. A possible substrate for dopamine-related changes in mood and behavior: prefrontal and limbic effects of a D3-preferring dopamine agonist. *Proc Natl Acad Sci U S A* 99:17113-17118. DOI: 10.1073/pnas.012260599 .

Black KJ, Koller JM, Campbell MC, Gusnard DA, and Bandak SI. 2010b. Quantification of indirect pathway inhibition by the adenosine A 2a antagonist SYN115 in Parkinson disease. *Journal of Neuroscience* 30:16284-16292. DOI: 10.1523/JNEUROSCI.2590-10.2010.

Black KJ, Koller JM, Snyder AZ, and Perlmutter JS. 2004. Atlas template images for nonhuman primate neuroimaging: Baboon and macaque. *Methods in Enzymology* 385:91-102. DOI: 10.1016/S0076-6879(04)85006-7.

Black KJ, Snyder AZ, Koller JM, Gado MH, and Perlmutter JS. 2001. Template images for nonhuman primate neuroimaging: 1. Baboon. *NeuroImage* 14:736-743. DOI: 10.1006/nimg.2001.0752 .

Desikan RS, Segonne F, Fischl B, Quinn BT, Dickerson BC, Blacker D, Buckner RL, Dale AM, Maguire RP, Hyman BT, Albert MS, and Killiany RJ. 2006. An automated labeling system for subdividing the

human cerebral cortex on MRI scans into gyral based regions of interest. *NeuroImage* 31:968-980. DOI: 10.1016/j.neuroimage.2006.01.021.

Fox PT, Mintun MA, Raichle ME, and Herscovitch P. 1984. A noninvasive approach to quantitative functional brain mapping with H2(15)O and positron emission tomography. *Journal of Cerebral Blood Flow and Metabolism* 4:329-333.

Henniger NE, Koller JM, Liou T, Matheson R, and Black KJ. 2009. Quantification of the temporal stability of arterial spin labeling functional magnetic resonance imaging. Washington University Undergraduate Research Symposium. St. Louis, Missouri, USA.

Herscovitch P, Markham J, and Raichle M. 1983. Brain blood flow measured with intravenous H 2 15 O. I. Theory and error analysis. *Journal of Nuclear Medicine* 24:782-789.

Lancaster JL, Woldorff MG, Parsons LM, Liotti M, Freitas CS, Rainey L, Kochunov PV, Nickerson D, Mikiten SA, and Fox PT. 2000. Automated Talairach atlas labels for functional brain mapping. *Human Brain Mapping* 10:120-131. DOI: http://www.talairach.org.

Ojemann JG, Akbudak E, Snyder AZ, McKinstry RC, Raichle M, and Conturo TE. 1997. Anatomic localization and quantitative analysis of gradient refocused echo-planar fMRI susceptibility artifacts. *NeuroImage* 6:156-167.

Raichle ME, Martin WR, Herscovitch P, Mintun MA, and Markham J. 1983. Brain blood flow measured with intravenous H2(15)O. II. Implementation and validation. *J Nucl Med* 24:790-798.

Siegel JS, Power JD, Dubis JW, Vogel AC, Church JA, Schlaggar BL, and Petersen SE. 2014. Statistical improvements in functional magnetic resonance imaging analyses produced by censoring high-motion data points. *Hum Brain Mapp* 35:1981-1996. DOI: 10.1002/hbm.22307.

Stewart SB, Koller JM, Campbell MC, and Black KJ. 2014. Arterial spin labeling versus BOLD in pharmacological fMRI. *PeerJ PrePrints*.

Taber KH, Black KJ, and Hurley RA. 2005. Blood flow imaging of the brain: 50 years experience. *Journal of Neuropsychiatry and Clinical Neurosciences* 17:441-446. DOI: 10.1176/appi.neuropsych.17.4.441.

Wang J, Licht DJ, Jahng GH, Liu CS, Rubin JT, Haselgrove J, Zimmerman RA, and Detre JA. 2003. Pediatric perfusion imaging using pulsed arterial spin labeling. *JMagn ResonImaging* 18:404-413.

Wang Z. 2012. Improving cerebral blood flow quantification for arterial spin labeled perfusion MRI by

removing residual motion artifacts and global signal fluctuations. *Magn Reson Imaging* 30:1409-1415. DOI: 10.1016/j.mri.2012.05.004.

PeerJ PrePrints | http://dx.doi.org/10.7287/peerj.preprints.464v3 | CC-BY 4.0 Open Access | rec: 11 Sep 2014, publ: 11 Sep 2014

Supplemental Material

Suppl. Table 1: Variability Across Subjects of Mean GM rCBF, WM rCBF and their Ratio

	Non-normalized Images	Multiplicatively Normalized	Additively Normalized
Mean GM rCBF (SD, CV) *	38.78 (7.51, 0.194)	62.02 (16.47, 0.266)	55.89 (8.11, 0.145)
Mean WM rCBF (SD, CV) *	27.56 (5.68, 0.206)	43.85 (11.54, 0.263)	44.67 (7.06, 0.159)
Mean GM:WM ratio (SD, CV)	1.416 (0.104, 0.074)	1.418 (0.102, 0.072)	1.256 (0.070, 0.056)

* Nominal units ml/hg/min

Suppl. Table 2: Within-Subject Variance in GM and WM

	Non-normalized Images	Multiplicatively Normalized	Additively Normalized
Within-subject GM SD* (CV) (mean across subjects)	6.48 (0.174)	7.54 (0.217)	12.77 (0.141)
Within-subject WM SD* (CV) (mean across subjects)	4.55 (0.171)	5.99 (0.211)	8.84 (0.140)

* Nominal units ml/hg/min

Suppl. Table 3: rCBF Changes in Visual Cortex and WM VOIs with Visual Stimulation

	Non-normalized Images	Multiplicatively Normalized	Additively Normalized
Mean change in rCBF (SD) in visual cortex region *	17.70 (13.88)	29.83 (18.91)	18.15 (13.37)
p	1.70×10^{-5}	1.03×10^{-6}	7.72×10^{-6}
Mean change in rCBF (SD) in white matter region *	1.07 (3.23)	2.85 (5.99)	1.53 (3.47)
p	0.15	0.05	0.06

* Nominal units ml/hg/min. Note that the mean changes are not strictly comparable between methods because of the multiplication. Hence we provide SD and p values for comparison.

PeerJ PrePrints | http://dx.doi.org/10.7287/peerj.preprints.464v3 | CC-BY 4.0 Open Access | rec: 11 Sep 2014, publ: 11 Sep 2014

Suppl. Figure 1: Determining the idealized mode.

The figure shows the frequency histogram for one of the CBF images. With this bin width, the true mode falls at 32 (frequency = 898, bin including all voxels with values 31.5–32.5), but the mean of the distribution and the vertex of the parabola shown (the idealized mode) both fall at 35.0.

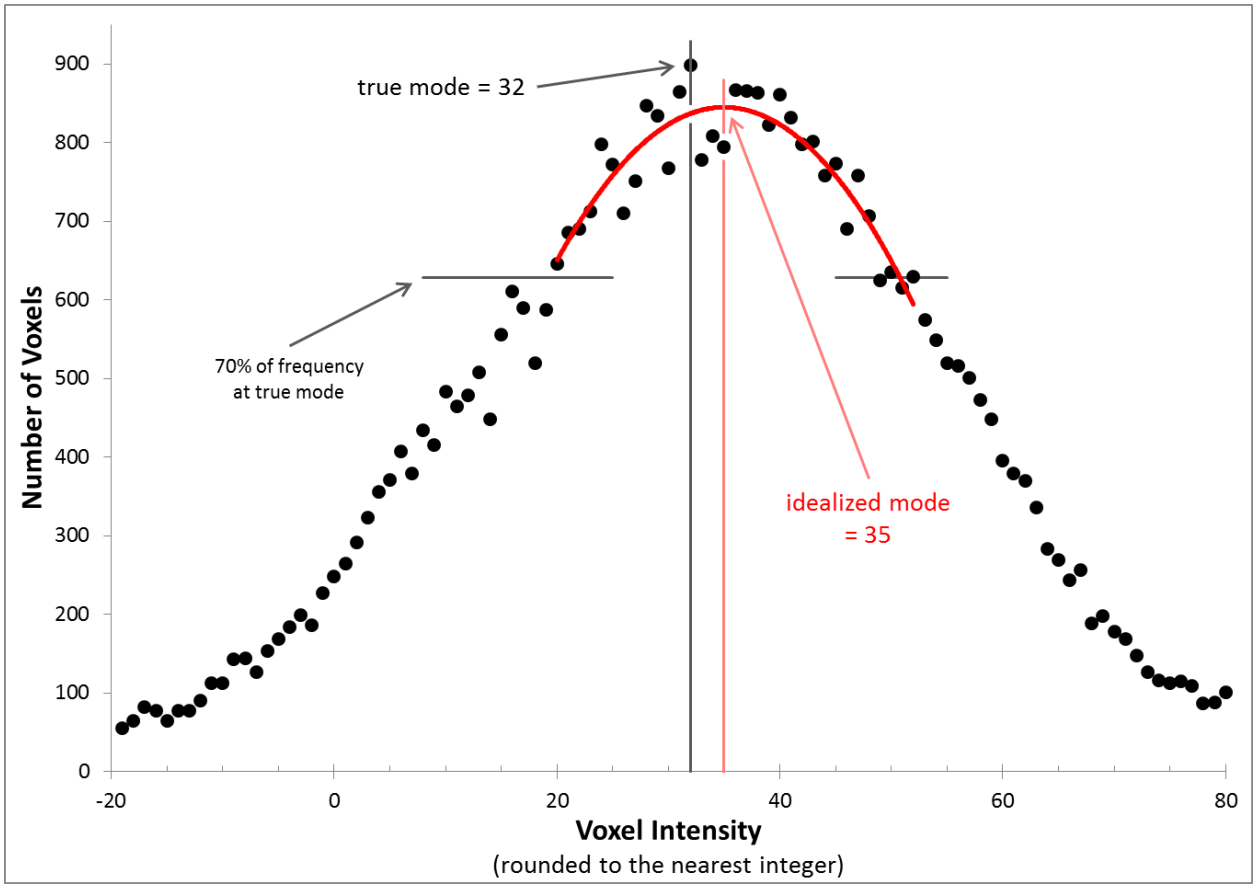

PeerJ PrePrints | http://dx.doi.org/10.7287/peerj.preprints.464v3 | CC-BY 4.0 Open Access | rec: 11 Sep 2014, publ: 11 Sep 2014